

Research Article

Received: October 11, 2023
Revised: December 11, 2023
Accepted: January 17, 2024

DOI: 10.60101/past.2024.251241

Thermal Efficiency of Solar Dryers for Drying Longan and Heat Transfer Modeling

Jagrapan Piwsaoad

Program of Physics, Faculty of Education, Loei Rajabhat University,
Loei – Chiang Khan Road, Mueang District, Loei Province 42000, Thailand
Corresponding Email: jagrapan25@gmail.com

Abstract

Longan drying in Loei Province, Thailand. There were two types of dryers with capacity in 5,000 kgs and 10 kgs of type 1 and 2, respectively. The moisture content of longans inside and outside the dryer; type 1 decreased from 80.91% (w.b.) to 20.0% (w.b.), the moisture content of longan samples outside the dryer decreased to 40.0% (w.b.) within 5 days; type 2 decreased from 80.91% (w.b.) to 22.0% (w.b.), the moisture content of longan samples outside the dryer decreased to 45.0% (w.b.) within 5 days respectively. Heat transfer modeling results showed that the moisture content calculated from the model corresponding to the measured values the $RMSE=0.5251$, 0.4266 and $R^2=0.9655$, 0.9745. The thermal efficiency of the dryer; type 1 has a thermal efficiency of 8.55%-25.27%; type 2 has a thermal efficiency of 4.42-26.11%.

Keywords: Solar Dryer, Longan, Heat Transfer Modeling, Thermal Efficiency

1. Introduction

Longan (*Dimocarpus longan*); Longan is one of the fruits that are found in large quantities in Thailand. Longan growing areas in Thailand are spread throughout every region. But there are a lot of them in the northern region. Longan production in 8 northern provinces, including Chiang Mai, Lamphun, Chiang Rai, Phayao, Lampang, Tak, Phrae, and Nan. In 2023, longan from 8 northern provinces has an area of 1,270,319 rai. Loei Province has an area of 35,677 rai of longan cultivation, and the yield each year is released at the same time and results in a low price.

Thailand is a country with suitable climate for agriculture because it is located in a zone with sufficient solar radiation for plant growth (1).

In many countries, agricultural products are naturally dried in the sun. However, with this method the product will be of low

quality and this method, longan will suffer a lot of damage due to rain, animals and insects that tends to occur during drying. To solve this problem a powerful dryer is required to dry longan. This is due to interference from external impurities and uneven drying rates. Many types of the solar dryers have been designed and developed in different parts of the world, providing different technical performance (2-5). Drying is possible even in adverse weather conditions and in any weather conditions. Working with solar energy, these dryers are the most cost-effective dryers. It is also easy to build and can store agricultural produce for a long time.

The objectives of this research were to investigate the performance of the two types solar dryer for drying longans and developed heat transfer modeling of solar dryer for drying longans. Finally, the thermal efficiency of the two types of the solar dryer was compared.

2. Materials and Experiment

2.1 Experimental Setup

Type 1 solar dryer was installed at Loei Province, Thailand. The dryer has a roof made of polycarbonate sheets on a concrete floor. The roof has a curved shape. The dryer is 24.0 m in length, 9.0 m in width and 4.0 m in height. Nine DC fans are installed on the rear. The fan is operated by two 50-W cell modules to exhaust air from the dryer.

The pictorial view of the dryer is shown in Figure 1. Longans inside the dryer are shown in Figure 2. The positions of all measurements and the schematic diagram showing heat and mass transfers are shown in Figure 3.



Figure 1 The solar dryer type 1



Figure 2 Longan inside the dryer type 1

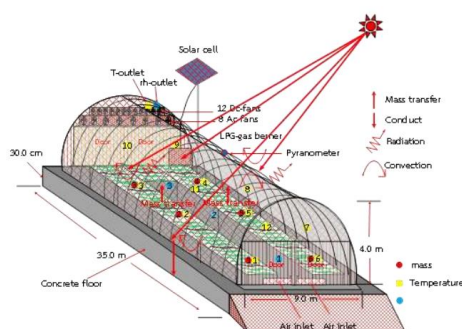


Figure 3 Measuring point of type1

Type 2 solar dryer was installed at Loei Province, Thailand. The dryer has a roof made of polycarbonate sheets on a metal sheet floor. The dryer is 2.0 m in width, 3.0 m in length and 2.0 m in height. To ventilate the dryer, two DC fans operated by 10-W solar cell modules were installed in the wall opposite to the air inlet. Two 300W heaters powered by AC electricity installed inside the solar collector, one biomass stove uses rubber wood as fuel.

The solar dryer, measuring points, longans inside the dryer and longans sample are shown in Figures 4-6.



Figure 4 The solar dryer type 2

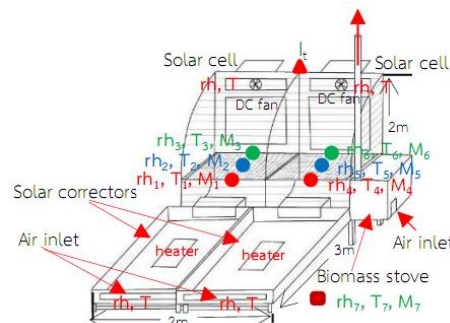


Figure 5 Measuring point of type 2

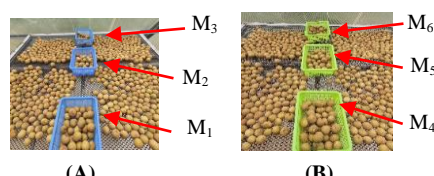


Figure 6 (A) Longan inside the dryer; tray1
(B) Longan inside the dryer; tray2

2.2 Experimental Procedure

In this study, longans were dried inside the solar dryer to investigate the dryer potential, research equipment is shown in Figure 7.

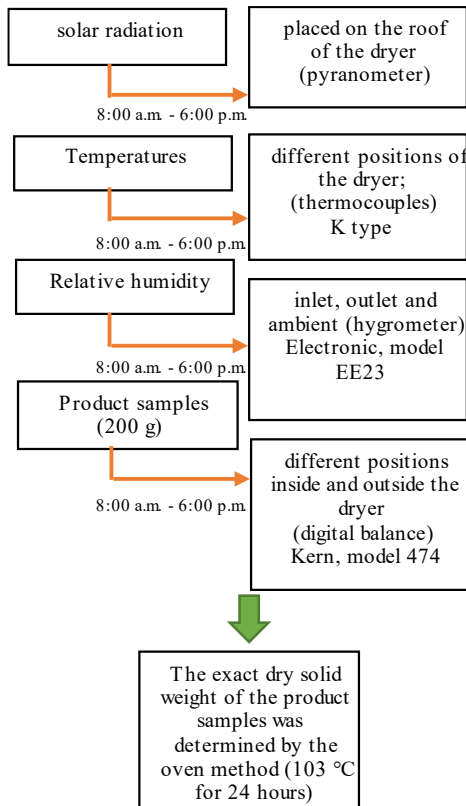


Figure 7 Research equipment

The moisture content during drying was estimated from the weight of the product samples and the estimated dried solid mass of the samples (6-7).

2.3 Heat Transfer Modeling

The heat transfer modeling consists of 5 equations; 1. energy balance of the cover, 2. energy balance of the air inside the dryer, 3. energy balance of the product, 4. energy balance on the floor and 5. mass balance equation. The details are as follows:

2.3.1 Energy Balance of the Cover

The energy balance of the cover is considered as: rate of accumulation of thermal energy in the cover, caused by various quantities

that affect the cover according to the equation (2.1) (8-10):

$$m_c c_{p,c} \left(\frac{dT_c}{dt} \right) = h_{c,c-a} (T_a - T_c) + A_c h_{r,c-s} (T_s - T_c) + A_c h_{w,c-amb} (T_{amb} - T_c) + h_{r,a-p} (T_p - T_a) + \alpha_c (T_c I_t A_c) \quad (2.1)$$

2.3.2 Energy Balance of the Air Inside the Dryer

This energy balance is the rate of accumulation of thermal energy in the air inside the dryer according to the equation (2.2) (8-10):

$$m_p c_p \left(\frac{dT_a}{dt} \right) = A_p h_{c,p-a} (T_f - T_a) + A_p h_{c,p-a} (T_p - T_a) + D_p A_p m_c c_p \alpha_p (T_p - T_a) \frac{dM_p}{dt} + (\rho_a v_a c_{p,c} T_a - \rho_a v_{in} c_{p,a} T_{in}) + U_c A_c (T_a - T_a) + [(1 - F_p)(1 - \alpha_f) + (1 - \alpha_p)F_p] I_t A_c \tau_c \quad (2.2)$$

2.3.3 Energy Balance of the Product

Rate of accumulation of thermal energy in the product according to the equation (2.3) (8-10):

$$m_c (c_{pg} + c_{pl} M_p) \frac{dT_p}{dt} = A_p (h_{c,p-a} (T_a - T_c) + A_p h_{r,p-c} (T_c - T_p) + D_p A_p \rho_p L_p + c_{pv} (T_a - T_p) \frac{dM_p}{dt} + F_p \alpha_p I_t A_c \tau_c) \quad (2.3)$$

2.3.4 Energy Balance on the Floor

Rate of accumulation of thermal energy in the floor according to the equation (2.4) (8-10):

$$m_f c_{p,f} \left(\frac{dT_f}{dt} \right) = A_f h_{c,f-a} (T_a - T_f) + A_f h_{r,f-un} (T_{un} - T_f) + (1 - F_p) \alpha_f I_t A_f \tau_c \quad (2.4)$$

2.3.5 Mass Balance Equation

The accumulation rate of moisture in the air inside dryer according to the equation (2.5) (8-10):

$$\rho_a v \frac{dH}{dt} = A_{in} \rho_a H_{in} v_{in} - A_{out} \rho_a H_{out} v_{out} + D_p A_p \rho_{d,p} \frac{dH}{dt} \quad (2.5)$$

From equation (2.1); m_c is mass of the cover (kg), $C_{p,c}$ is specific heat of cover ($\text{Jkg}^{-1}\text{K}^{-1}$), T_c is the cover temperature (K), $h_{c,c-a}$ is convective heat transfer coefficient between the cover and the air in the greenhouse dryer ($\text{Wm}^{-2}\text{K}^{-1}$), T_a is the drying air temperature (K), A_c is the cover area (m^2), $h_{r,c-s}$ is radiative heat transfer coefficient between the cover and the sky ($\text{Wm}^{-2}\text{K}^{-1}$), T_s is the sky temperature (K), $h_{w,c-amb}$ is convective heat transfer coefficient between the cover and ambient air due to wind ($\text{Wm}^{-2}\text{K}^{-1}$), T_{amb} is the ambient temperature (K), α_c is the absorptance of the cover (decimal), I_t is the solar radiation (Wm^{-2}).

From equation (2.2); m_p is mass of the product (kg), C_p is specific heat of air in the product ($\text{Jkg}^{-1}\text{K}^{-1}$), A_p is product area (m^2), $h_{c,p-a}$ is convective heat transfer coefficient between the product and the drying air ($\text{Wm}^{-2}\text{K}^{-1}$), T_f is temperature of the floor (K), D_p is the average distance between the cover and the product (m), α_p is the absorptance of the product (decimal), T_p is temperature of the product (K), M_p is the moisture content of product in the dryer model (db, decimal), α_a is density of air (kgm^{-3}), V_{out} is outlet air flow rate (m^3s^{-1}), C_{p-a} is specific heat of air in the product ($\text{Jkg}^{-1}\text{K}^{-1}$), T_{out} is temperature of the air at the outlet of the dryer (K), V_{in} is inlet air flow rate (m^3s^{-1}), T_{in} is temperature of the air at the inlet air of the dryer (K), U_c is overall heat loss coefficient from the cover to ambient air ($\text{Wm}^{-2}\text{K}^{-1}$), F_p is fraction of solar radiation falling on the product (decimal), α_f is absorptance of the floor (decimal), τ_c is transmittance of the cover (decimal).

From equation (2.3); m_p is mass of product (kg), C_{pg} is the specific heat of air in the dryer ($\text{Jkg}^{-1}\text{K}^{-1}$), C_{pl} is the specific heat of liquid in the product ($\text{Jkg}^{-1}\text{K}^{-1}$), ρ_p is density of product (kgm^{-3}), L_p is the latent heat of evaporation of the product ($\text{Jkg}^{-1}\text{K}^{-1}$).

From equation (2.4) m_f is mass of floor (kg), $h_{D,f-un}$ is conductive heat transfer between the floor and the underground ($\text{Wm}^{-2}\text{K}^{-1}$), C_{pf} is specific heat of floor ($\text{Jkg}^{-1}\text{K}^{-1}$), T_{un} is ground temperature (K).

From equation; (2.5) v is speed of the air (ms^{-1}), A_{in} total cross-sectional area of the air inlets (m^2), A_{out} is total cross-sectional area of the air outlets (m^2), H is humidity ratio (kgkg^{-1}),

H_{in} is humidity ratio of air entering the dryer (kgkg^{-1}), H_{out} is humidity ratio of the air leaving the dryer (kgkg^{-1}) and $\rho_{d,p}$ is density of the dried product (kgm^{-3}).

2.3.6 Solution Procedure

The system of equations (2.1 to 2.5) is solved numerically using the finite difference technique. On the basis of the drying air temperature and relative humidity inside the dryer. This system of equations is a set of implicit calculations for the time interval Δt . These are solved by the Gauss-Jordan elimination method using the recorded values for the drying air temperature and relative humidity, the change in moisture content of the product (ΔM) for the given time interval. The numerical solution was programmed as shown in Figure 8.

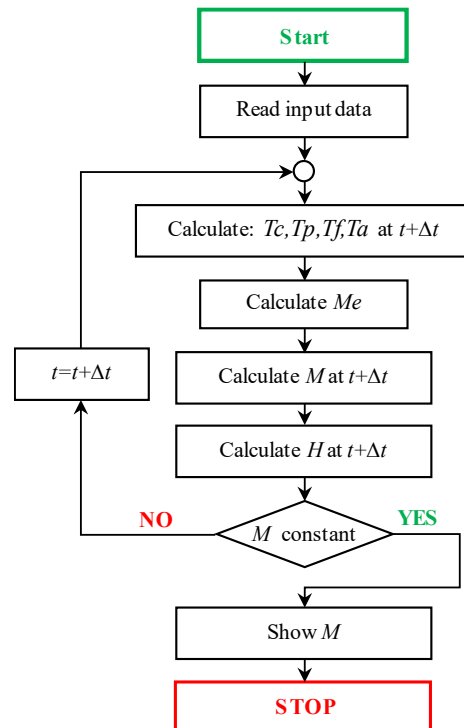


Figure 8 The numerical solution program

The process is repeated until the final time is reached. The numerical solution was programmed in Compaq Visual FORTRAN. Performance Analysis, three statistical parameters were used for performance analysis. Root means square error $RMSE$ and

determination coefficient R^2 of agreement were computed to estimate the overall model performance.

2.4 The Thermal Efficiency of the Solar Dryer

The thermal efficiency was calculated from the drying rate to the energy yield rate for longans drying is determined by (11):

$$\eta = [(\dot{m}_w h_{fg}) / (A_{solar} I_t)] \times 100(\%) \quad (2.6)$$

Where η is the thermal efficiency (%), \dot{m}_w is the evaporation rate of water (kg/s), h_{fg} is the latent heat of vaporization of water (kJ/kg), I_t is the total radiation incident on the dryer (Wm^{-2}), A_{solar} is the solar radiation area of the dryer (m^2).

3. Results and Discussion

3.1 Drying Characteristic of Longans

The experimental results are shown in Table 1.

Table 1 The average solar radiation with time

| Time (hr.) | Solar radiation (Wm^{-2}) |
|------------|--------------------------------------|
| 1 | 81.00 |
| 2 | 99.11 |
| 3 | 119.55 |
| 4 | 420.48 |
| 5 | 575.78 |
| 6 | 777.00 |
| 7 | 625.27 |
| 8 | 545.14 |
| 9 | 250.91 |
| 10 | 105.21 |
| 11 | 81.25 |

The results of the experiment found that the average solar radiation intensity was 81.00 to 777.00 (Wm^{-2}).

The average temperature during the drying are shown in Table 2.

Table 2 The average temperature during the drying

| Temperature (°C) | Type 1 | Type 2 |
|------------------|--------|--------|
| front | 56.87 | 43.51 |
| middle | 57.53 | 45.72 |
| behind | 57.48 | 45.64 |
| air inlet | 26.87 | 26.47 |
| air outlet | 55.51 | 45.57 |

The results of the experiment found that Type 1 has a temperature measured at various positions: front 56.87°C, center 57.53°C, behind 57.48°C, air inlet 26.87°C, air outlet 55.51°C; type 2, front 43.51°C, center 45.72°C, behind 45.64°C, air intake 26.47°C, air outlet 45.57°C.

The average relative humidity during drying are shown in Table 3.

Table 3 The average relative humidity during drying

| Relative humidity (%) | Type | |
|-----------------------|--------|--------|
| | Type 1 | Type 2 |
| front | 47.22% | 59.17% |
| middle | 45.15% | 58.36% |
| behind | 48.95% | 58.79% |
| air inlet | 76.77% | 76.77% |
| air outlet | 60.11% | 62.37% |

The average relative humidity at various positions type 1; front 47.22%, middle 45.15%, behind 48.95%, air inlet 76.77%, air outlet 60.11%. Type 2; front 59.17%, middle 58.36%, behind 58.79%, air inlet 76.77%, air outlet 62.37 %.

The average moisture content of longan are shown in Table 4.

Table 4 The average moisture content of longan

| Temperature (°C) | Type | |
|------------------|-------------|-------------|
| | Type 1 | Type 2 |
| M ₁ | 80.67-20.00 | 80.67-23.22 |
| M ₂ | 80.23-20.13 | 80.23-22.13 |
| M ₃ | 80.88-21.22 | 80.91-22.42 |
| M ₄ | 80.17-20.14 | 80.17-22.00 |
| M ₅ | 80.91-21.22 | 80.61-22.22 |
| M ₆ | 80.82-22.26 | 80.71-22.26 |
| M _{ab} | 80.91-40.00 | 80.91-45.00 |

The average moisture content of longan inside and outside the dryer; type 1 and type 2 decreased from an initial value of 80.91%(w.b.) to a final value of 20.0%(w.b.) and 22.0%(w.b.) within 5 days, while the moisture content of outside the dryer sample decreased remaining 40.0%(w.b.) and 45.0%(w.b.) during the same period.

Longans have a structure of 3 layers: the outer shell (hard and brown in color), the flesh (jelly-like and white) and the innermost layer, the seed (hard and brown in color). Therefore, most of the evaporation of water in

longan occurs in the second layer and out to the outer shell. Therefore, the reducing behavior of water (the moisture content) therefore decreases slowly. The moisture content of both types of the dryers at different positions, there is a difference equal to 0.74% (w.b.).

3.2. Heat Transfer Modeling

The comparison results from the measurement and the modeling found that type 1 and type 2 are shown in Figures 9 and 10.

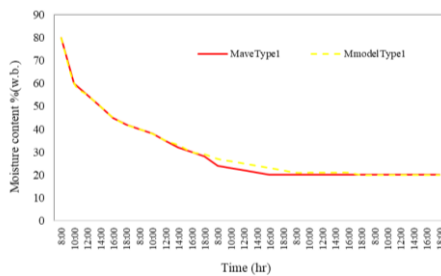


Figure 9 Comparison results from the measurement and the modeling type 1

The comparison results from the measurement and the modeling moisture content are type 1; $RMSE=0.5251$ and $R^2=0.9655$.

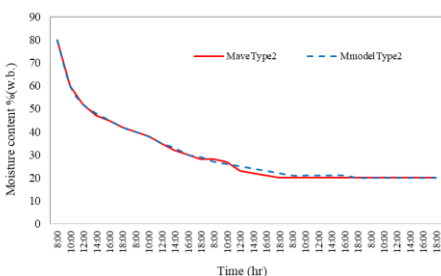


Figure 10 Comparison results from the measurement and the modeling type 2

The comparison results from the measurement and the modeling moisture content are type 2; $RMSE=0.4266$ and $R^2=0.9745$.

3.3 Thermal Efficiency of Solar Dryer

The thermal efficiency of type 1 and type 2 solar dryers are shown in Table 5 and Figure 11.

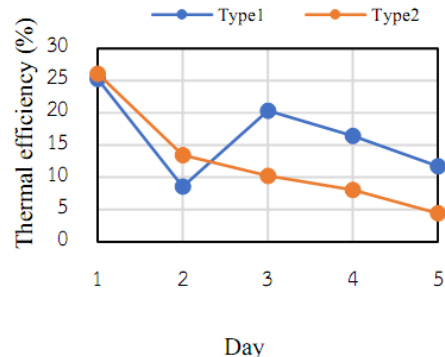


Figure 11 Comparison of thermal efficiency

Table 5 Thermal efficiency of the solar dryer

| Thermal efficiency (%) | Model | |
|------------------------|--------|--------|
| | Type 1 | Type 2 |
| Day1 | 25.27 | 26.11 |
| Day2 | 8.55 | 13.45 |
| Day3 | 20.37 | 10.22 |
| Day4 | 16.45 | 8.06 |
| Day5 | 11.75 | 4.420 |

The thermal efficiency of the solar dryer for longan drying calculated per day, type 1 was found to be between 8.55-25.27%. type 2 was found to be between 4.42-26.11%.

4. Conclusions

The results of drying longans using a solar dryer showed that both types of longans were of good quality.

The moisture content of longan inside and outside the dryer; type 1 and type 2 decreased from an initial value of 80.91% (w.b.) to a final value of 20.0% (w.b.) and 22.0% (w.b.) within 5 days, while the moisture content of outside the dryer sample decreased remaining 40.0% (w.b.) and 45.0% (w.b.) during the same period; when compared with research using other types of dryers, it was found that they had similar characteristics (12-14).

The model predicts well the variation of the moisture content during the drying. The overall comparison of the simulated moisture content is type 1; $RMSE=0.5251$ and $R^2=0.9655$, type 2; $RMSE=0.4266$ and $R^2=0.9745$ respectively.

The thermal efficiency of solar dryer for drying longans calculated per day found that

type 1 has a thermal efficiency of 8.55-25.27%. Type 2 has a thermal efficiency of 4.42-26.11%.

The results of longan drying using different sized dryers do not indicate that the size of the dryer determines the efficiency. In this research, it was found that the amount of solar radiation intensity is an important factor.

The advantage of type 1 is that it can be dried in large quantities and has a consistent temperature at every point. energy. The advantage of type 2 is that there are 3 sources of energy, including solar energy. Thermal energy from heaters and energy from biomass can be used in all weather conditions and all seasons.

Acknowledgements

The author would like to thank Program of Physics, Faculty of Education, Loei Rajabhat University for the financial support provided for this research work.

Declaration of Conflicting Interests

The authors declared that they have no conflicts of interest in the research, authorship, and this article's publication.

References

1. Janjai S, Laksanaboonsong J, Thongsathiya A. Development of a method for generating operational solar radiation maps from satellite data for a tropical environmental. *Solar Energy*. 2005;78:739-51.
2. Duffie JA, Beckman WA. *Solar Engineering of thermal Processes*. John Wiley and sons, New York., 1991.
3. Sulaiman MA. Review of solar dryer for agricultural and marine products. *Renewable and sustainable Energy Reviews*. 2010;14:1-30.
4. Murthy MV. A review of new technologies, models and experimental investigations of solar dryers. *Renewable Energy Reviews*. 2009;13:835-44.
5. Sharma A, Chem CR, Lan NV. Solar-energy drying systems. A review *Renewable and Sustainable Energy Reviews*. 2009;13:1185-210.
6. Piwsaoad J. Hybrid solar dryer for drying pineapples of raimoung community enterprise, Loei Province, Thailand. *Life Sci Environ J*. 2019;20(1):97-110.
7. Piwsaoad J, Phusampao C. Factors Affecting Mangos Drying. *J Sci Technol*. 2021;13(2):80-5.
8. Janjai S, Lamert N, Intawee P, Mahayothee B, Bala BK, Nagle M, Muller J. Experimental and simulated performance of a PV-ventilated solar greenhouse dryer for drying of peeled longan and banana, *Solar Energy*. (83) (2009) 1550-65.
9. Janjai S, Khamvongsa V, Bala BK. Development, design and performance of a PV-Ventilated Greenhouse Dryer. *Int Energy J*. 2007;8:249-58.
10. Janjai S, Lamert N, Intawee P, Mahayothee B, Bala BK, Nagle M, Muller J. Experimental and simulated performance of a PV-ventilated solar greenhouse dryer for drying of peeled longan and banana. *Solar Energy*. 2009;83:1550-65.
11. Piwsaoad J, Phusampao C. Performance of the Solar Dyer and Moisture Content Prediction of Sweet Tamarind Using an ANN. *Life Sci Environ J*. 2023;24(2):285-96.
12. Agricultural Statistics of Thailand. 2023, Ministry of Agriculture & Co-Operatives, Bangkok, Thailand.
13. Han MM, Yi Y, Wang H X, Huang F. Investigation of the maillard reaction between polysaccharides and proteins from longan pulp and the improvement in activities. *Molecules*. 2017;22(938):1-14.
14. Somjai C, Siriwaharn T, Kulprachakarn K, Chaipoot S, Phongphisutthinant R, Wiriyacharee P. Utilization of Maillard reaction in moist-dry-heating system to enhance physicochemical and antioxidative properties of dried whole longan fruit. *Heliyon*. 2021;7(5), Article e07094. <https://doi.org/10.1016/j.heliyon.2021.e07094>.